Free Energy and Solvent Dependence of Intramolecular Electron Transfer in Donor-Substituted Re(I) Complexes

ARTICLE *in* JOURNAL OF THE AMERICAN CHEMICAL SOCIETY · JANUARY 1991

Impact Factor: 12.11

2 AUTHORS:

D. Brent Macqueen

SRI International

39 PUBLICATIONS **1,136** CITATIONS

SEE PROFILE

Kirk S Schanze

University of Florida

328 PUBLICATIONS **11,389** CITATIONS

SEE PROFILE

thermodynamically less stable than the corresponding alkenyl and alkyl esters.

Experimental Section

A. Preparation of 1-Propynyl Tosylate.[1] Phenyl(propynyl)iodonium tosylate[1] (5.0 g, 12 mmol) was decomposed in a solution of silver tosylate (0.1 g) in CH_2Cl_2 (50 mL). Decomposition was complete in 3 h. The solvent was removed in vacuo, and the residue was taken up in CH_2Cl_2/hexanes, filtered, concentrated, and chromatographed on silica gel (15 g). The column was eluted first with hexanes and followed with 10%, 20%, and 50% CH_2Cl_2 in hexanes. The fractions containing the product were combined and concentrated to give an oil (0.81 g, 32% yield), which solidified upon cooling (10 °C). The product was then recrystallized several times from hot pentane (mp 21 °C). X-ray quality crystals were obtained by slowly cooling a concentrated solution of propynyl tosylate in pentane to -20 °C.

B. Preparation of Ethynyl Benzoate. (Phenylethynyl)iodonium triflate[44] (3.78 g, 10 mmol) was dissolved in 50 mL of methylene chloride and cooled to 0 °C in an ice-water bath. A solution of sodium benzoate (5.76 g, 40 mmol) in 40 mL of water was added, and the mixture was stirred vigorously for 2 min. The organic phase was separated, and the aqueous phase was extracted with additional methylene chloride. The combined organic phase was dried over $MgSO_4$ and concentrated. The resulting oil was chromatographed on silica. The column was eluted at first with hexanes followed with 20% CH_2Cl_2 in hexanes. The fractions containing ethyl benzoate were combined and concentrated. The resulting solid was then recrystallized from pentane to give 0.59 g (40% yield) of product. A concentrated solution of ethynyl benzoate in pentane at room temperature was cooled to -20 °C to yield X-ray quality crystals.

(44) Stang, P. J.; Arif, A. M.; Crittell, C. M. *Angew. Chem., Int. Ed. Engl.* **1990**, *29*, 287.

Acknowledgment. Financial support by the National Cancer Institute of NIH (Grant 2R01CA16903) at Utah and by the US-Israel Binational Science Foundation (BSF) and the Fund for the Promotion of Science at the Technion in Israel are gratefully acknowledged.

Registry No. 4, 94957-44-5; **5**, 130468-62-1; **6**, 113779-41-2; **7**, 135074-94-1; **8**, 135074-95-2; **9**, 135074-96-3; **10**, 123812-75-9; **11**, 83313-98-8; **12**, 123812-74-8; **13**, 135074-97-4; **14**, 135074-98-5; phenyl(propynyl)iodonium tosylate, 94957-41-2; phenyl(ethynyl)iodonium triflate, 125803-61-4.

Supplementary Material Available: Details of the X-ray crystal and structural data for compounds **4** and **5** (25 pages); listing of calculated and observed structure factors for **4** and **5** (8 pages). Ordering information is given on any current masthead page.

Free Energy and Solvent Dependence of Intramolecular Electron Transfer in Donor-Substituted Re(I) Complexes

D. Brent MacQueen and Kirk S. Schanze*

Contribution from the Department of Chemistry, University of Florida, Gainesville, Florida 32611. *Received April 22, 1991. Revised Manuscript Received June 10, 1991*

Abstract: A comprehensive investigation of photoinduced intramolecular electron transfer (ET) in a series of six complexes of the type *fac*-(b)$Re^{I}(CO)_3$-D (where b is a diimine ligand and D is a dimethylaniline electron donor) is reported. Photoexcitation of the $d\pi$ (Re) $\rightarrow \pi^*$ (diimine) metal-to-ligand charge-transfer excited state initiates a sequence of forward and back ET reactions:

$$(b)Re^{I}(CO)_3\text{-}D \xrightarrow{h\nu} (b^-)Re^{II}(CO)_3\text{-}D \xrightarrow[\Delta G_{FET}]{k_{FET}} (b^-)Re^{I}(CO)_3\text{-}D^+ \xrightarrow[\Delta G_{BET}]{k_{BET}} (b)Re^{I}(CO)_3\text{-}D$$

The driving force for forward and back ET (ΔG_{FET} and ΔG_{BET}, respectively) is varied by changing the electron demand of the diimine ligand. Cyclic voltammetry and steady-state emission studies were carried out for each complex in three solvents (CH_2Cl_2, DMF, and CH_3CN) to allow estimation of ΔG_{FET} and ΔG_{BET}. The forward ET reactions are weakly exothermic (-0.5 eV < ΔG_{FET} < -0.1 eV) and the back ET reactions are highly exothermic (-2.6 eV < ΔG_{BET} < -1.5 eV). Rates for forward ET (k_{FET}) for each of the complexes in the three solvents were determined by using time-resolved emission spectroscopy. The forward ET rate ranges from 10^7 s^{-1} to $>10^9$ s^{-1} and is strongly dependent on ΔG_{FET} and solvent polarity. The dependence of k_{FET} on ΔG_{FET} is consistent with nonadiabatic semiclassical Marcus theory. The solvent dependence of k_{FET} suggests that the reorganization energy increases with solvent polarity in a manner that is consistent with the Marcus-Hush dielectric continuum model. Rates for back ET (k_{BET}) were determined by using laser flash photolysis in two solvents. The back ET rate ranges from 10^7 s^{-1} to 5×10^8 s^{-1} and is not solvent dependent. Interestingly, k_{BET} displays a weak, inverted dependence on ΔG_{BET}. Analysis of the rate data using a multimode quantum mechanical expression suggests that a possible explanation for the weak free-energy dependence may be that metal complex-based high-frequency acceptor modes are coupled to the back ET process.

Introduction

The importance of electron transfer (ET) in a variety of chemical, biological, and physical processes has stimulated much interest in the factors that control ET between molecular sites.[1-4] Studies have examined the effects of free energy (ΔG_{ET}),[1-3,5-9] donor-acceptor electronic coupling,[1,2,10-37] and medi-

(1) For recent reviews of ET reactions in chemical and biological systems, see: (a) Marcus, R. A.; Sutin, N. *Biochim. Biophys. Acta* **1985**, *811*, 265. (b) Newton, M. D.; Sutin, N. *Annu. Rev. Phys. Chem.* **1984**, *35*, 437. (c) DeVault, D. *Quantum Mechanical Tunnelling in Biological Systems*, 2nd ed.; Cambridge University Press: New York, 1984. (d) *Tunnelling in Biological Systems*; Chance, B., DeVault, D. C., Frauenfelder, H., Marcus, R. A., Schrieffer, J. R., Sutin, N., Eds.; Academic Press: New York, 1979. (e) *Electron Transfer in Biology and the Solid State*; Johnson, M. K., King, R. B., Kurtz, D. M., Jr., Kutal, C., Norton, M. L., Scott, R. A., Eds. *Adv. Chem. Sci.* **1990**, *No. 226*.

(2) For a compilation of reviews, see: *Prog. Inorg. Chem.* **1983**, *30*, 1-528.

(3) For reviews of early work on ET, see: (a) Zwolinski, B. J.; Marcus, R. A.; Eyring, H. *Chem. Rev.* **1955**, *55*, 157. (b) Marcus, R. A. *Annu. Rev. Phys. Chem.* **1964**, *15*, 155.

(4) *Photoinduced Electron Transfer*, Parts A-D; Fox, M. A., Chanon, M., Eds.; Elsevier: Amsterdam, 1988.

(5) Mok, C. Y.; Zanella, A. W.; Creutz, C.; Sutin, N. *Inorg. Chem.* **1984**, *23*, 2891.

(6) Rehm, D.; Weller, A. *Isr. J. Chem.* **1970**, *8*, 259.

(7) Bock, C. R.; Connor, J. A.; Guitierrez, A. R.; Meyer, T. J.; Whitten, D. G.; Sullivan, B. P.; Nagle, J. K. *J. Am. Chem. Soc.* **1979**, *101*, 4815.

(8) Miller, J. R.; Beitz, J. V. *J. Chem. Phys.* **1981**, *74*, 6746.

(9) Miller, J. R.; Beitz, J. V.; Huddleston, R. K. *J. Am. Chem. Soc.* **1984**, *106*, 5057.

0002-7863/91/1513-7470$02.50/0

Scheme I

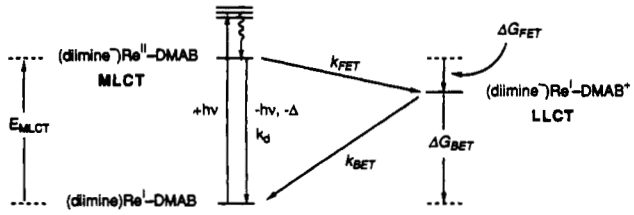

um[1,2,11,15b,16,17c,38-53] on the rate of ET (k_{ET}). Recent investigations have verified the inverted dependence of k_{ET} on ΔG_{ET} for highly exothermic reactions,[9,10,54-58] and demonstrated that long-range ET occurs between molecular sites that are separated by large distances on the molecular scale.[1,9-20]

Chromophore–quencher (C–Q) molecules, which contain a covalently linked donor–acceptor pair, have been the focus of many investigations concerning the mechanism of ET.[59,60] Photochemical excitation of the acceptor (or donor) in a C–Q compound initiates a sequence that begins with forward ET to produce a charge-transfer state, followed by back ET in the charge-transfer state to regenerate the ground state. In most C–Q compounds, forward ET is moderately exothermic and back ET is strongly exothermic, and as a result, these systems provide a convenient tool to study ET in the Marcus "normal" and "inverted" free-energy regions. Studies of organic C–Q systems have provided important findings which include: demonstration of the inverted region effect;[55] proof that rapid long-range ET occurs across extended networks of σ-bonds;[11] development of molecules which mimick the photosynthetic reaction center by efficiently achieving long-lived, photoinduced charge separation;[61,62] and evidence for bridge-mediated "superexchange" coupling between donor and acceptor sites.[21,63]

By comparison, fewer studies have been carried out on C–Q compounds that contain a transition metal chromophore.[17,56,57,64-67]

(10) Closs, G. L.; Calcaterra, L. T.; Green, N. J.; Penfield, K. W.; Miller, J. R. *J. Phys. Chem.* **1986**, *90*, 3673.

(11) (a) Paddon-Row, M. N.; Oliver, A. M.; Warman, J. M.; Smit, K. J.; De Haas, M. P.; Oevering, H.; Verhoeven, J. W. *J. Phys. Chem.* **1988**, *92*, 6958. (b) Warman, J. M.; Smit, K. J.; de Haas, M. P.; Jonker, S. A.; Paddon-Row, M. N.; Oliver, A. M.; Kroon, J.; Oevering, H.; Verhoeven, J. W. *J. Phys. Chem.* **1991**, *95*, 1979.

(12) Antolovich, M.; Keyte, P. J.; Oliver, A. M.; Paddon-Row, M. N.; Kroon, J.; Verhoeven, J. W.; Jonker, S. A.; Warman, J. M. *J. Phys. Chem.* **1991**, *95*, 1933.

(13) (a) Isied, S. S.; Vassilian, A.; Magnuson, R. H.; Schwarz, H. A. *J. Am. Chem. Soc.* **1985**, *107*, 7432. (b) Isied, S. S.; Vassilian, A.; Wishart, J. F.; Creutz, C.; Schwarz, H. A.; Sutin, N. *J. Am. Chem. Soc.* **1988**, *110*, 635. (c) Vassilian, A.; Wishart, J. F.; van Hemelryck, B.; Schwarz, H.; Isied, S. S. *J. Am. Chem. Soc.* **1990**, *112*, 7278.

(14) (a) Faraggi, M.; DeFelippis, M. R.; Klapper, M. H. *J. Am. Chem. Soc.* **1989**, *111*, 5141. (b) Faraggi, M.; DeFelippis, M. R.; Klapper, M. H. *J. Am. Chem. Soc.* **1990**, *112*, 5640.

(15) (a) Finckh, P.; Heitele, H.; Volk, M.; Michel-Beyerle, M. E. *J. Phys. Chem.* **1988**, *92*, 6584. (b) Heitele, H.; Finckh, P.; Weeren, S.; Pollinger, F.; Michel-Beyerle, M. E. *J. Phys. Chem.* **1989**, *93*, 5173.

(16) (a) Leland, B. A.; Joran, A. D.; Felker, P. M.; Hopfield, J. J.; Zewail, A. H.; Dervan, P. B. *J. Phys. Chem.* **1985**, *89*, 5571. (b) Joran, A. R.; Leland, B. A.; Felker, P. M.; Zewail, A. H.; Hopfield, J. J.; Dervan, P. B. *Nature* **1987**, *327*, 508.

(17) (a) Schanze, K. S.; Sauer, K. *J. Am. Chem. Soc.* **1988**, *110*, 1180. (b) Schanze, K. S.; Cabana, L. A. *J. Phys. Chem.* **1990**, *94*, 2740. (c) Perkins, T. A.; Hauser, B. T.; Eyler, J. R.; Schanze, K. S. *J. Phys. Chem.* **1990**, *94*, 8745. (d) MacQueen, D. B.; Perkins, T. A.; Schanze, K. S. *Mol. Cryst. Liq. Cryst.* **1991**, *94*, 8745.

(18) Wasielewski, M. R.; Niemczyk, M. P.; Johnson, D. G.; Svec, W. A.; Minsek, D. W. *Tetrahedron* **1989**, *45*, 4785.

(19) For reviews of ET in proteins, see: (a) Gray, H. B. *Aldrichchim. Acta* **1990**, *23*, 87. (b) Mayo, S. L.; Ellis, W. R., Jr.; Crutchley, R. J.; Gray, H. B. *Science* **1986**, *233*, 948.

(20) McLendon, G. *Acc. Chem. Res.* **1988**, *21*, 160.

(21) Rodriguez, J.; Kirmaier, C.; Johnson, M. R.; Freisner, R. A.; Holten, D.; Sessler, J. L. *J. Am. Chem. Soc.* **1991**, *113*, 1652.

(22) Meyer, T. J. In ref 2, p 389.

(23) Stein, C. A.; Lewis, N. A.; Seitz, G. *J. Am. Chem. Soc.* **1982**, *104*, 2596.

(24) Richardson, D. E.; Taube, H. *J. Am. Chem. Soc.* **1983**, *105*, 40.

(25) Balaji, V.; Jordan, K. D.; Burrow, P. D.; Paddon-Row, M. N.; Patney, H. K. *J. Am. Chem. Soc.* **1982**, *104*, 6849.

(26) McManis, G. E.; Nielson, R. M.; Gochev, A.; Weaver, M. J. *J. Am. Chem. Soc.* **1989**, *111*, 5533.

(27) McConnell, H. M. *J. Chem. Phys.* **1961**, *35*, 508.

(28) Hoffman, R. *Acc. Chem. Res.* **1971**, *4*, 1.

(29) Ohta, L.; Closs, G. L.; Morokuma, K.; Green, N. *J. Am. Chem. Soc.* **1986**, *108*, 1319.

(30) Larsson, S.; Volosov, A. *J. Chem. Phys.* **1986**, *85*, 2548.

(31) Plato, M.; Mobius, K.; Michel-Beyerle, M. E.; Bixon, M.; Jortner, J. *J. Am. Chem. Soc.* **1988**, *110*, 7279.

(32) (a) Siddarth, P.; Marcus, R. A. *J. Phys. Chem.* **1990**, *94*, 2985. (b) Siddarth, P.; Marcus, R. A. *J. Phys. Chem.* **1990**, *94*, 8430.

(33) (a) Beratan, D. N.; Hopfield, J. J. *J. Am. Chem. Soc.* **1984**, *106*, 1584. (b) Beratan, D. *J. Am. Chem. Soc.* **1986**, *108*, 4321.

(34) Hupp, J. T. *J. Am. Chem. Soc.* **1990**, *112*, 1563.

(35) (a) Marcus, R. A. *Chem. Phys. Lett.* **1987**, *133*, 471. (b) Marcus, R. A. *Chem. Phys. Lett.* **1988**, *146*, 13.

(36) Christensen, H. E. M.; Conrad, L. S.; Mikkelsen, K. V.; Nielsen, M. K.; Ulstrup, J. *Inorg. Chem.* **1990**, *29*, 2808.

(37) Newton, M. D. *J. Phys. Chem.* **1988**, *92*, 3049.

(38) (a) Marcus, R. A. *J. Chem. Phys.* **1956**, *24*, 966. (b) Marcus, R. A. *J. Chem. Phys.* **1965**, *43*, 679.

(39) Hush, N. S. *Trans. Faraday Soc.* **1961**, *57*, 557.

(40) (a) Powers, M. J.; Meyer, T. J. *J. Am. Chem. Soc.* **1978**, *100*, 4393. (b) Powers, M. J.; Meyer, T. J. *J. Am. Chem. Soc.* **1980**, *102*, 1289.

(41) (a) Brunschwig, B. S.; Ehrenson, S.; Sutin, N. *J. Phys. Chem.* **1986**, *90*, 3657. (b) Brunschwig, B. S.; Ehrenson, S.; Sutin, N. *J. Phys. Chem.* **1987**, *91*, 4714.

(42) (a) Suppan, P. *Chimia* **1988**, *42*, 320. (b) Suppan, P. *J. Photochem. Photobiol. A: Chem.* **1990**, *50*, 293.

(43) Closs, G. L.; Miller, J. R. *Science* **1988**, *240*, 440.

(44) Schmidt, J. A.; Liu, J.-Y.; Bolton, J. R.; Archer, M. D.; Gadzekpo, V. P. Y. *J. Chem. Soc., Faraday Trans. 1* **1989**, *85*, 1027.

(45) Gennett, T.; Milner, D. F.; Weaver, M. J. *J. Phys. Chem.* **1985**, *89*, 2787.

(46) Gaines, G. L., III; O'Neill, M. P.; Svec, W. A.; Niemczyk, M. P.; Wasielewski, M. R. *J. Am. Chem. Soc.* **1991**, *113*, 719.

(47) Simon, J. D.; Su, S. G. *J. Chem. Phys.* **1987**, *87*, 7016.

(48) Kahlow, M. A.; Jarzeba, W.; Kang, T. J.; Barbara, P. F. *J. Chem. Phys.* **1989**, *90*, 151.

(49) Hynes, J. T. *J. Phys. Chem.* **1986**, *90*, 3701.

(50) Rips, I.; Jortner, J. *J. Chem. Phys.* **1987**, *87*, 2090.

(51) Bashkin, J. S.; McLendon, G. In ref 1e, p 147.

(52) Hoffman, B. M.; Ratner, M. A. *J. Am. Chem. Soc.* **1987**, *109*, 6237.

(53) Brunschwig, B. S.; Sutin, N. *J. Am. Chem. Soc.* **1989**, *111*, 7454.

(54) Miller, J. R.; Calcaterra, L. T.; Closs, G. L. *J. Am. Chem. Soc.* **1984**, *106*, 3947.

(55) Wasielewski, M. R.; Niemczyk, M. P.; Svec, W. A.; Pewitt, E. B. *J. Am. Chem. Soc.* **1985**, *107*, 1080.

(56) Chen, P.; Duesing, R.; Tapolsky, G.; Meyer, T. J. *J. Am. Chem. Soc.* **1989**, *111*, 8305.

(57) Fox, L. S.; Kozik, M.; Winkler, J. R.; Gray, H. B. *Science* **1990**, *247*, 1069.

(58) (a) Gould, I. R.; Ege, D.; Moser, J. E.; Farid, S. *J. Am. Chem. Soc.* **1990**, *112*, 4290. (b) Gould, I. R.; Young, R. H.; Moody, R. E.; Farid, S. *J. Phys. Chem.* **1991**, *95*, 2068.

(59) For recent reviews, see: (a) *Covalently Linked Donor-Acceptor Species for Mimicry of Photosynthetic Electron and Energy Transfer*; Gust, D., Moore, T. A., Eds.; *Tetrahedron* **1989**, *45*, 4669. (b) Wasielewski, M. R. In ref 4, Part A, p 161.

(60) *The Exciplex*, Gordon, M., Ware, W., Eds.; Academic Press: New York, 1975.

(61) (a) Gust, D.; Moore, T. A.; Moore, A. L.; Barrett, D.; Harding, L. O.; Making, L. R.; Liddell, P. A.; DeSchryver, F. C.; Van der Auweraer, M.; Bensasson, R. V.; Rougee, M. *J. Am. Chem. Soc.* **1988**, *110*, 321. (b) Gust, D.; Moore, T. A.; Moore, A. L.; Makings, L. R.; Seely, G. R.; Ma, X.; Trier, T. T.; Gao, F. *J. Am. Chem. Soc.* **1988**, *110*, 7567.

(62) (a) Wasielewski, M. R.; Niemczyk, M. P.; Svec, W. A.; Pewitt, E. B. *J. Am. Chem. Soc.* **1985**, *107*, 5562. (b) Wasielewski, M. R.; Gaines, G. L., III; O'Neill, M. P.; Svec, W. A.; Niemczyk, M. P. *J. Am. Chem. Soc.* **1990**, *112*, 4559.

(63) Wasielewski, M. R.; Niemczyk, M. P.; Johnson, D. G.; Svec, W. A.; Minsek, D. W. In ref 59a, p 4785.

(64) (a) Chen, P.; Westmoreland, T. D.; Danielson, E.; Schanze, K. S.; Anthon, D.; Neveaux, P. E., Jr.; Meyer, T. J. *Inorg. Chem.* **1987**, *26*, 1116. (b) Meyer, T. J. *Acc. Chem. Res.* **1989**, *22*, 163. (c) Chen, P.; Danielson, E.; Meyer, T. J. *J. Phys. Chem.* **1988**, *92*, 3708. (d) Chen, P.; Curry, M.; Meyer, T. J. *Inorg. Chem.* **1989**, *28*, 2271.

(65) Danielson, E.; Elliott, C. M.; Merkert, J. W.; Meyer, T. J. *J. Am. Chem. Soc.* **1987**, *109*, 2519.

For example, to date, the rates for both forward and back ET have only been quantitatively determined in two transition-metal-based C–Q systems.[17c,57] Despite the fact that less work has been carried out on transition-metal C–Q compounds, these systems are attractive for use in studies of intramolecular ET because the driving force for both forward and back ET (ΔG_{FET} and ΔG_{BET}, respectively) can be easily varied by changing ligands on the metal center.[17] The efficacy of this approach was underscored by a recent study of back ET in a series of donor-substituted Re(I)–diimine complexes.[56]

In the present paper we report the results of a study of the rates of forward and back ET in the series of donor-substituted complexes, (b)ReDMAB. (In this acronym, b = a diimine ligand and DMAB refers to the *N,N*-dimethylaminobenzoate electron donor; see structures below for ligand abbreviations.) In these complexes, photoexcitation of the $d\pi$ (Re) $\rightarrow$ π^* (b) metal-to-ligand charge-transfer (MLCT) excited state initiates the sequence of forward and back ET reactions shown in Scheme I. The (b)-$Re^I(CO)_3$– chromophore was selected for this study for several reasons. First, the Re $\rightarrow$ diimine MLCT state is luminescent, thereby allowing k_{FET} to be determined by using time-resolved emission spectroscopy. Second, ΔG_{FET} and ΔG_{BET} can be varied by changing the electron demand of the diimine ligand. Forward and back ET rates were determined in the (b)ReDMAB series as a function of ΔG_{ET} in solvents of varying polarity. The rate of the weakly exothermic forward reaction displays a driving force dependence that is consistent with semiclassical ET theory. By contrast, the strongly exothermic back reaction displays an inverted dependence of rate on driving force; however, analysis of the back ET rate/free-energy correlation indicates that the free-energy dependence of the reaction is weaker than observed in other systems.[54,55,57,58] This study provides the first example of a metal complex C–Q system in which k_{FET} and k_{BET} are available for a wide range of ΔG_{ET} and in solvents of varying polarity.

Experimental Section

General Synthetic. Solvents and chemicals used for synthesis were of reagent grade and used without purification unless noted. 2,2′-Bipyridine, 4,4′-dimethyl-2,2′-bipyridine, and 2,2′-bipyrazine (Aldrich) were used as received. The other substituted bipyridine ligands (tmb, dab, deb) were prepared and purified by literature procedures.[68,69] Silica gel (Merck, 230–400 mesh) and neutral alumina (Fisher, Brockman activity grade III) were used for chromatography. ^1H and ^{13}C NMR spectra were recorded on a GE QE-300 spectrophotometer.

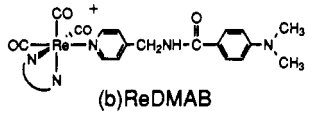

(b)ReDMAB

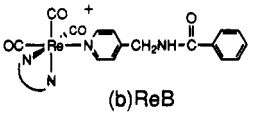

(b)ReB

Diimine Ligands and Abbreviations

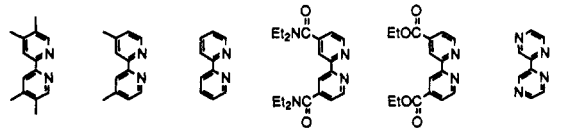

tmb dmb bpy dab deb bpz

***N*-Benzoyl-4-(aminomethyl)pyridine.** Benzoyl chloride (5.0 g, 35 mmol) was added dropwise to a mixture of 4-aminomethylpyridine (3.8 g, 35 mmol) in 100 mL of 5% $NaOH/H_2O$. The solid amide was filtered from the solution, dried, and then recrystallized from ethanol. The product was obtained as white crystals, yield 4.5 g (55%). Spectral data: ^1H NMR (DMSO) δ 4.50 (d, 2 H), 7.30 (d, 2 H), 7.45–7.60 (m, 5 H), 7.91 (d, 2 H), 9.14 (t, 1 H).

***N*-(4-Pyridyl)methyl-*N'*,*N'*-dimethylaminobenzamide.** *N,N*-Dimethylaminobenzoyl chloride hydrochloride[70] (6.6 g, 30 mmol) and triethylamine (7.1 g, 75 mmol) were dissolved in 50 mL of CH_2Cl_2. 4-Aminomethylpyridine (3.2 g, 30 mmol) was then added dropwise and the resulting solution was stirred overnight. The CH_2Cl_2 solution was filtered, washed with 0.1 M Na_2CO_3, and dried over Na_2SO_4; then the solvent was evaporated. Recrystallization from ethanol produced a pale yellow crystalline product, yield 3.3 g (43%). Spectral data: ^1H NMR (DMSO) δ 2.98 (s, 6 H), 4.47 (d, 2 H), 6.73 (d, 2 H), 7.29 (d, 2 H), 7.81 (d, 2 H), 8.51 (d, 2 H), 8.79 (t, 1 H).

General Procedure for Preparation of (diimine)Re(CO)$_3$Cl Complexes. $Re(CO)_5Cl$ was prepared by photolysis of a CO-purged CCl_4 solution of $Re_2(CO)_{10}$ by using a Hanovia medium-pressure Hg arc in a quartz immersion well. The $Re(CO)_5Cl$ was purified by recrystallization from $EtOH/H_2O$. Approximately 250 mg of $Re(CO)_5Cl$ and 1 equiv of the diimine ligand were dissolved in 100 mL of toluene and the solution was heated at reflux for 1 h. Upon cooling, the (diimine)$Re(CO)_3Cl$ precipitated and the yellow or orange product was collected by filtration on a sintered glass filter and dried. The yield was typically 70–90%, based on $Re(CO)_5Cl$.

General Procedure for Preparation of (b)ReB and (b)ReDMAB Complexes. Approximately 250 mg of (diimine)$Re(CO)_3Cl$, 3 equiv of $AgPF_6$, and 3 equiv of the substituted pyridine ligand were dissolved in a minimum volume of DMF (5–10 mL) and the resulting solution was heated to 70 °C. During this time the reaction was monitored by TLC (silica gel, 5% $MeOH/CH_2Cl_2$). When the reaction was complete (typically 30–40 min), the solution was cooled, the DMF was evaporated, and the product was then dissolved in 50 mL of CH_2Cl_2. The solid AgCl precipitate was removed by filtration and the CH_2Cl_2 was then evaporated.

Purification was effected by repeated chromatography on silica gel eluting with 5% $MeOH/CH_2Cl_2$, except for (bpz)ReDMAB and (bpz)-ReB which were purified by chromatography on alumina eluting with 20% CH_3CN/CH_2Cl_2. The typical yield after chromatography was 20%.

(tmb)ReB. Spectral data: ^1H NMR ($CDCl_3$) δ 2.44 (s, 6 H), 2.49 (s, 6 H), 4.54 (d, 2 H), 7.24 (d, 2 H), 7.33–7.50 (m, 5 H), 7.83 (d, 2 H), 7.83 (d, 2 H), 7.91 (d, 2 H), 8.05 (s, 2 H), 8.67 (s, 2 H).

(tmb)ReDMAB. Spectral data: ^1H NMR (acetone-d_6) δ 2.48 (s, 6 H), 2.50 (s, 6 H), 2.91 (s, 6 H), 4.46 (d, 2 H), 6.59 (d, 2 H), 7.26 (d, 2 H), 7.30 (t, 1 H), 7.70 (d, 2 H), 7.96 (d, 2 H), 8.17 (s, 2 H), 8.69 (s, 2 H).

(dmb)ReB. Spectral data: ^1H NMR ($CDCl_3$) δ 2.61 (s, 6 H), 4.59 (d, 2 H), 7.40–7.60 (m, 5 H), 7.80 (d, 2 H), 7.88 (d, 2 H), 8.39 (t, 1 H), 8.44 (d, 2 H), 8.59 (s, 2 H), 9.25 (d, 2 H).

(dmb)ReDMAB. Spectral data: ^1H NMR (acetone-d_6) δ 2.62 (s, 6 H), 2.89 (s, 6 H), 4.54 (d, 2 H), 6.72 (d, 2 H), 7.38 (d, 2 H), 7.75 (d, 2 H), 7.79 (d, 2 H), 8.09 (t, 1 H), 8.42 (d, 2 H), 8.58 (s, 2 H), 9.25 (d, 2 H).

(bpy)ReB. Spectral data: ^1H NMR (acetone-d_6) δ 4.57 (d, 2 H), 7.38–7.57 (m, 5 H), 7.83–7.88 (m, 2 H), 7.93–8.00 (m, 2 H), 8.48–8.57 (m, 5 H), 8.71 (d, 2 H), 9.44 (d, 2 H).

(bpy)ReDMAB. Spectral data: ^1H NMR (acetone-d_6) δ 3.00 (s, 6 H), 4.51 (d, 2 H), 6.70 (d, 2 H), 7.36 (d, 2 H), 7.73 (d, 2 H), 7.97 (m, 2 H), 8.07 (t, 1 H), 8.42 (m, 4 H), 8.71 (d, 2 H), 9.44 (d, 2 H).

(dab)ReB. Spectral data: ^1H NMR (acetone-d_6) δ 1.08 (t, 6 H), 1.19 (t, 6 H), 3.27 (q, 4 H), 3.53 (q, 4 H), 4.57 (d, 2 H), 7.6–7.9 (m, 5 H), 7.87 (d, 2 H), 7.93 (d, 2 H), 8.38 (t, 1 H), 8.49 (d, 2 H), 8.75 (s, 2 H), 9.51 (d, 2 H).

(dab)ReDMAB. Spectral data: ^1H NMR ($CDCl_3$) δ 1.11 (t, 6 H), 1.29 (t, 6 H), 3.02 (s, 6 H), 3.44 (q, 4 H), 3.68 (q, 4 H), 4.55 (d, 2 H), 6.63 (d, 2 H), 6.90 (t, 1 H), 7.28 (d, 2 H), 7.63 (d, 2 H), 7.72 (d, 2 H), 8.06 (d, 2 H), 8.25 (s, 2 H), 9.09 (d, 2 H).

(deb)ReB. Spectral data: ^1H NMR (CD_3CN) δ 1.59 (t, 6 H), 4.54–4.63 (m, 6 H), 7.34 (d, 2 H), 7.53–7.72 (m, 5 H), 7.86 (d, 2 H), 8.23 (d, 2 H), 8.32 (d, 2 H), 9.02 (s, 2 H), 9.47 (d, 2 H).

(deb)ReDMAB. Spectral data: ^1H NMR ($CDCl_3$) δ 1.51 (t, 6 H), 3.00 (s, 6 H), 4.56 (m, 6 H), 6.64 (d, 2 H), 6.90 (t, 1 H), 7.22 (d, 2 H), 7.72 (d, 2 H), 7.89 (d, 2 H), 8.57 (d, 2 H), 8.76 (d, 2 H), 9.62 (s, 2 H).

(bpz)ReB. Spectral data: ^1H NMR (acetone-d_6) δ 4.59 (d, 2 H), 7.48–7.59 (m, 5 H), 7.88 (d, 2 H), 8.42 (t, 1 H), 8.55 (d, 2 H), 9.22 (d, 2 H), 9.58 (d, 2 H), 10.14 (s, 2 H).

(bpz)ReDMAB. Spectral data: ^1H NMR (acetone-d_6) δ 3.02 (s, 6 H), 4.53 (d, 2 H), 6.72 (d, 2 H), 7.48 (d, 2 H), 7.75 (d, 2 H), 8.10 (t, 1 H), 8.52 (d, 2 H), 9.23 (d, 2 H), 9.58 (d, 2 H), 10.14 (s, 2 H).

Electrochemistry. Cyclic voltammetry was carried out on a BAS CV-2 voltammograph. Experiments were conducted in a one-compartment cell which contained Pt disk working, Pt wire auxilliary, and SSCE reference

(66) (a) Elliott, C. M.; Freitag, R. A.; Blaney, D. D. *J. Am. Chem. Soc.* **1985**, *107*, 4647. (b) Cooley, L. F.; Headford, C. G. L.; Elliott, C. M.; Kelley, D. F. *J. Am. Chem. Soc.* **1988**, *110*, 6673.

(67) Schemhl, R. H.; Ryu, C. K.; Elliott, C. M.; Headford, C. L. E.; Ferrere, S. *In ref 1e*, p 211.

(68) Munavali, S.; Gratzel, M. *Chem. Ind.* **1987**, 724.

(69) Cook, M. J.; Lewis, A. P.; McAuliffe, G. S. G.; Skarda, V.; Thomsen, A. J.; Glaspar, J. L.; Robbins, D. J. *J. Chem. Soc., Perkin Trans. 2* **1984**, 1293.

(70) Munakata, K.-I.; Tanaka, S.; Toyoshima, S. *Chem. Pharm. Bull.* **1980**, *28*, 2045.

Table I. Electrochemical Data for (b)ReDMAB Complexes[a]

	CH_3CN[b]		DMF[b]		CH_2Cl_2[c]	
ligand	$E_{1/2}(D/D^+)$[d]	$E_{1/2}(b/b^-)$	$E_{p,a}(D/D^+)$[e]	$E_{1/2}(b/b^-)$	$E_{1/2}(D/D^+)$[d]	$E_{1/2}(b/b^-)$
tmb	0.994	−1.387	1.186	−1.313	1.150	−1.422
dmb	1.002	−1.245	1.175	−1.154	1.168	−1.271
bpy	0.964	−1.164	1.134	−1.056	1.140	−1.140
dab	0.952	−1.001	1.144	−0.928	1.136	−0.914
deb	0.990	−0.667	1.196	−0.540	1.145	−0.607
bpz	0.989	−0.717	1.165	−0.554	1.067	−0.520

[a] All potentials in volts versus SSCE (+0.236 versus NHE). [b] 0.1 M tetrabutylammonium hexafluorophosphate supporting electrolyte. [c] 0.1 M tetrabutylammonium perchlorate supporting electrolyte. [d] $E_{1/2}(D/D^+)$ is the half-wave potential for the DMAB/DMAB$^+$ couple. [e] $E_{p,a}(D/D^+)$ is the peak potential for the irreversible DMAB anodic wave.

electrodes. Tetrabutylammonium perchlorate (TBAP, recrystallized three times from ethanol) at a concentration of 0.1 M was used as a supporting electrolyte. The temperature-dependent experiments were carried out by a literature procedure.[71]

Luminescence Measurements. Solvents used in emission experiments were spectrophotometric grade. Samples were thoroughly degassed by bubbling argon through the solutions for 30 min. Steady-state emission spectroscopy was conducted on a Spex F-112A spectrophotometer. Emission spectra were corrected for instrument response with correction factors generated in-house by using a 1000-W tungsten primary standard lamp. Sample concentrations for steady-state emission were $\approx 2 \times 10^{-5}$ M. Emission decay experiments were carried out by using time-correlated single photon counting on a commercially available system (Photochemical Research Associates).[72] Sample concentrations for emission decay experiments were $\approx 5 \times 10^{-6}$ M. Stern–Volmer quenching experiments indicated that this concentration was sufficiently low to preclude lifetime quenching by bimolecular pathways. Emission lifetimes were determined from computer fits of the decay using a computer program which allowed for deconvolution of the excitation lamp profile. The fits were judged satisfactory by $\chi^2 \leq 1.3$ and by random scatter in the residual plots.

Nanosecond Transient Absorption Spectroscopy. The transient absorption experiments were conducted at the Center for Fast Kinetics Research in Austin, TX, on a system that has been described in the literature.[73] The samples were excited by using the third harmonic of a Nd:YAG for excitation (355 nm, 6 ns fwhm, 8 mJ/pulse).

The decay rate constants were determined from fits of the transient absorption kinetic data using a computer program which allowed for multiexponential (rise and) decay processes. For most of the complexes the transient absorption kinetics were satisfactorily fitted using a single exponential decay function, but in cases where forward ET was comparatively slow (e.g., (tmb)ReDMAB/CH_3CN and (dmb)ReDMAB/CH_3CN), inclusion of a rise component in the fitting function improved the fit. In these cases, the reported lifetimes are the decay lifetime component. Note that while inclusion of the rise component improved the quality of the fit, the lifetime of the decay component was the same within experimental error (±15%) as obtained from a fit using a single exponential decay function.

Results and Discussion

Structure of the Donor-Substituted Complexes. Molecular modeling studies were carried out using (bpy)ReDMAB as a structural model for the series. The SYBYL program (Tripos force field) was utilized in the modeling studies.[74] The atomic coordinates for the (bpy)Re(CO)$_3$(pyridine) moiety were obtained from the crystal structure of the structurally similar complex [(bpy)Re(CO)$_3$(*N*-methyl-4,4′-bipyridinium)][PF$_6$]$_2$.[64d] The methylamide-linked DMAB donor site was constructed and the geometry was energy-optimized using the MAXMIN algorithm. The main degrees of conformational freedom for the complex are rotation around the single bonds between the methylene group and the 4-pyridyl carbon and the methylene group and the amide nitrogen. By using the SEARCH algorithm of SYBYL, the range of energetically accessible conformations which result from rotation around these bonds was determined for (bpy)ReDMAB. The conformational search indicates that rotation around the two single bonds is relatively unhindered (many conformations are available within 2 kcal of the minimum energy conformer); however, for the entire set of accessible conformations, the separation distance between the Re atom and the center of the DMAB ring remains within the range 9.0–10.5 Å. Figure 1 shows three superimposed structures in which the DMAB unit is in three typical energetically accessible conformations. The modeling studies indicate that, under the conditions at which the ET kinetics were determined, the separation distance between the metal complex and the donor is relatively constrained, but the orientation of the DMAB unit with respect to the complex is unconstrained and very likely fluctuates rapidly on the timescale of the ET process.

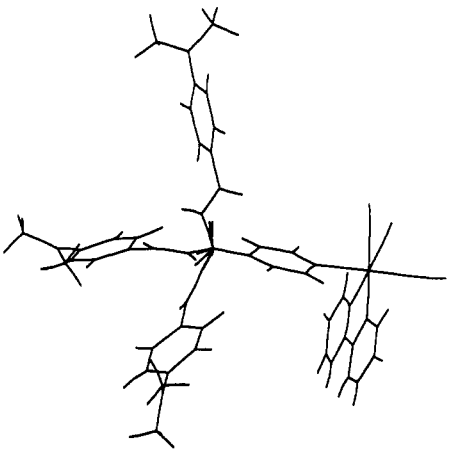

Figure 1. Projection of the three-dimensional structure of (bpy)ReDMAB generated by using the SYBYL molecular modeling program. Three structures are superimposed which differ with respect to the conformation of the rotatable bonds defined in the text. These structures illustrate the range of orientations which are accessible to the DMAB donor group.

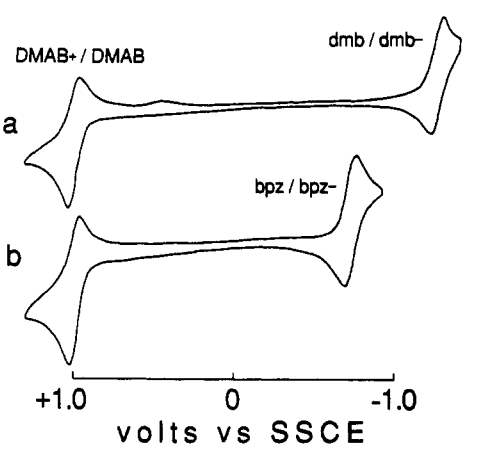

Figure 2. Cyclic voltammograms for (b)ReDMAB complexes in CH_3CN solution with 0.1 M TBAP electrolyte and SSCE reference electrode: (a) (dmb)ReDMAB, (b) (bpz)ReDMAB.

Electrochemistry and Emission of the (b)ReL Complexes: Thermodynamics of Intramolecular Electron Transfer. Cyclic voltammetry was carried out on CH_3CN, DMF, and CH_2Cl_2

(71) Yee, E. L.; Cave, R. J.; Guyer, K. L.; Tyma, P. D.; Weaver, M. J. *J. Am. Chem. Soc.* **1979**, *101*, 1131.
(72) Perkins, T. A.; Pourreau, D. B.; Netzel, T. L.; Schanze, K. S. *J. Phys. Chem.* **1989**, *93*, 4511.
(73) Atherton, S. J.; Beaumont, P. C. *J. Phys. Chem.* **1987**, *91*, 3993.
(74) Clark, M.; Cramer, R. D., III; Van Openbosch, N. *J. Comput. Chem.* **1989**, *10*, 982.

Table II. Emission Data for (b)ReB and (b)ReDMAB Complexes[a]

	CH_3CN			DMF			CH_2Cl_2/TBAP[b]		
diimine	$E_{max}(E_{0,0})$	τ_B	τ_{DMAB}	$E_{max}(E_{0,0})$	τ_B	τ_{DMAB}	$E_{max}(E_{0,0})$	τ_B	τ_{DMAB}
tmb	18 400 (2.57)	1450	46	18 300 (2.58)	1080	14	18 800 (2.60)	2180	5.5
dmb	17 400 (2.45)	269	18	17 100 (2.43)	159	6.5	17 900 (2.51)	597	1.9
bpy	16 900 (2.38)	211	11	16 800 (2.38)	115	4.7	17 500 (2.45)	456	1.4
dab	16 100 (2.30)	107	4.9	15 900 (2.27)	57	2.7	16 700 (2.32)	194	0.8
deb	15 300 (2.15)	75	0.4	14 800 (2.11)	31	0.5	15 900 (2.23)		<0.5
bpz	14 600 (2.08)	27	1.0	14 000 (2.03)	12	1.3	15 000 (2.12)		<0.5

[a] E_{max} is the emission maximum in cm^{-1} and $E_{0,0}$ is the estimated 0–0 emission energy in eV units. $E_{0,0}$ is approximated from computer fits of the corrected emission spectra of (b)ReB (ref 75). τ_B and τ_{DMAB} are the emission lifetimes of the (b)ReB and (b)ReDMAB complexes, respectively, in nanoseconds. Error in lifetimes less than 10 ns is estimated as ±10%. Less than 5% error is expected in lifetimes which are greater than 10 ns. [b] TBAP = tetrabutylammonium perchlorate, 0.1 M.

Table III. Forward Electron-Transfer Data for (b)ReDMAB Complexes[a]

	CH_3CN				DMF		CH_2Cl_2/TBAP	
ligand	ΔG_{FET}	k_{FET}	$\Delta H^{\ddagger}_{FET}$, kcal	$\Delta S^{\ddagger}_{FET}$, eu	$\approx\Delta G_{FET}$[b]	k_{FET}	ΔG_{FET}	k_{FET}
tmb	−0.19	2.1 (0.1) × 10^7	3.3 (0.2)	−14 (2)	−0.08	7.0 (0.4) × 10^7	−0.03	1.8 (0.3) × 10^8
dmb	−0.20	5.0 (0.4) × 10^7	3.5 (0.2)	−12 (2)	−0.10	1.5 (0.3) × 10^8	−0.07	5.2 (0.5) × 10^8
bpy	−0.22	8.6 (0.4) × 10^7	3.0 (0.2)	−12 (2)	−0.19	2.0 (0.3) × 10^8	−0.17	7.1 (0.6) × 10^8
dab	−0.35	1.9 (0.3) × 10^8	2.3 (0.2)	−13 (2)	−0.20	3.5 (0.4) × 10^8	−0.27	1.2 (0.3) × 10^9
deb	−0.49	2.5 (0.3) × 10^9			−0.37	2.0 (0.3) × 10^9	−0.48	
bpz	−0.37	9.6 (0.5) × 10^8			−0.31	6.8 (0.5) × 10^8	−0.53	

[a] ΔG_{FET} in eV and k_{FET} in s^{-1}. Estimated error in k_{FET}, $\Delta H^{\ddagger}_{FET}$, and $\Delta S^{\ddagger}_{FET}$ given in parentheses. [b] ΔG_{FET} in DMF is approximate because DMAB/$DMAB^+$ couple is irreversible.

Table IV. Transient Absorption Decay Rates: MLCT Decay for (b)ReB Complexes and Back Electron-Transfer Rates for (b)ReDMAB Complexes[a]

	(b)ReB, τ_{TA}[b]		(b)ReDMAB					
			CH_3CN			CH_2Cl_2/TBAP		
ligand	CH_3CN	CH_2Cl_2/TBAP	ΔG_{BET}	τ_{TA}[b]	k_{BET}[c]	ΔG_{BET}	τ_{TA}[b]	k_{BET}[c]
tmb	1450	2130	−2.38	213	4.7 × 10^6	−2.57	463	2.2 × 10^6
dmb	283	615	−2.25	120	8.3 × 10^6	−2.44	284	3.6 × 10^6
bpy	219	464	−2.13	77	1.3 × 10^7	−2.28	194	5.3 × 10^6
dab	111	205	−1.95	53	1.9 × 10^7	−2.05	111	9.1 × 10^6
deb	75	186	−1.66	28	3.6 × 10^7	−1.75	42	2.4 × 10^7
bpz	26	46	−1.71			−1.59	27	3.7 × 10^7

[a] Units: lifetimes in ns, rate constants in s^{-1}, and ΔG_{BET} in eV. Estimated errors: τ_{TA} (±15%), k_{BET} (±15%), ΔG_{BET} (±25 mV). [b] Transient absorption decay lifetime. [c] Back ET rate constant, calculated by the equation: $k_{BET} = 1/\tau_{TA}$.

solutions of the (b)ReDMAB complexes. The electrochemical response was qualitatively similar for each complex; representative voltammograms are shown in Figure 2 and the relevant potentials are listed in Table I. Anodic sweeps reveal a wave at $E_{1/2} \approx +1.0$–$+1.2$ V which is reversible in CH_3CN and CH_2Cl_2 and irreversible in DMF. This wave is assigned to oxidation of the electron donor, $E_{1/2}$(DMAB/$DMAB^+$); observation of an anodic wave at $E_{1/2} = +0.90$ V for a CH_3CN solution of the model compound, *N,N*-diethyl-*p*-(*N'N'*-dimethylamino)benzamide, supports this assignment. Cathodic scans reveal a reversible wave with $E_{1/2}$ that depends on the diimine ligand; this wave is assigned to reduction of the diimine ligand, $E_{1/2}(b/b^-)$. The data in Table I show that $E_{1/2}$(DMAB/$DMAB^+$) is relatively constant and $E_{1/2}(b/b^-)$ varies widely over the series. Note that in each solvent, $E_{1/2}(b/b^-)$ follows the sequence, tmb < dmb < bpy < dab < bpz < deb; this ordering is a direct result of the effect of the substituents on the π^* LUMO energy of the diimine ligand.

The temperature dependence of $E_{1/2}$(DMAB/$DMAB^+$) and $E_{1/2}$(bpy/bpy^-) for (bpy)ReDMAB in CH_3CN solution was determined by using nonisothermal electrochemistry in order to estimate ΔS_{ET} for the heterogenous ET processes.[71] The $E_{1/2}$ values were determined over the range −10° to +45 °C and the ΔS_{ET} values, calculated from the temperature-dependent data, are 13.5 ± 2 and 9.6 ± 2 eu, for the bpy/bpy^- and $DMAB^+$/DMAB couples, respectively.

The emission of the (b)ReL complexes was studied in CH_3CN, DMF, and CH_2Cl_2/TBAP solutions. The (b)ReB model complexes produce a broad, structureless emission band with a maximum (E_{max}) that ranges from approximately 18 500 cm^{-1} (b = tmb) to 14 500 cm^{-1} (b = bpz) (Table II). Identical emission bands are observed for the corresponding (b)ReDMAB complexes; however, the intensity of the emission is much weaker owing to the occurence of forward ET (vide infra). The 0–0 emission energies ($E_{0,0}$) for the (b)ReB complexes, estimated by computer fits of the emission spectra,[75] are also listed in Table II. The emission observed from both series of complexes is assigned to the $d\pi$ (Re) → π^* (diimine) MLCT excited state on the basis of several lines of evidence. First, similar broad, structureless MLCT emission has been observed from a variety of structurally related (diimine)$Re^I(CO)_3L$ complexes.[75,76] Second, in accord with the MLCT assignment E_{max} decreases as $E_{1/2}(b/b^-)$ becomes less negative (see Tables I and II).[77]

The thermodynamic driving force for forward and back ET in the (b)ReDMAB complexes (refer to Scheme I for definition of the thermodynamic quantities) can be estimated from the electrochemical and emission data listed in Tables I and II by using the following equations:[42,78]

$$\Delta G_{FET} \approx E_{1/2}(\text{DMAB/DMAB}^+) - E_{1/2}(b/b^-) - E_{0,0} \quad (1)$$

$$\Delta G_{BET} \approx E_{1/2}(b/b^-) - E_{1/2}(\text{DMAB/DMAB}^+) \quad (2)$$

In eq 1 and 2, $E_{1/2}$ values are from cyclic voltammetry and $E_{0,0}$ is the energy of the relaxed MLCT excited state. The ΔG_{FET} and

(75) Caspar, J. V. Ph.D. Dissertation, University of North Carolina at Chapel Hill, 1983.
(76) Wrighton, M.; Morse, D. L. *J. Am. Chem. Soc.* **1974**, *96*, 998.
(77) Dodsworth, E. S.; Lever, A. B. P. *Chem. Phys. Lett.* **1986**, *124*, 152.
(78) The Coulombic stabilization energy (CSE) is neglected because when the +1 charge on the metal complex is considered, forward and back ET are charge-shift reactions. In any case, the CSE term will be constant for the series of (b)ReDMAB complexes, and therefore its neglect will not affect the relative ΔG_{FET} and ΔG_{BET} values.

ΔG_{BET} values in CH_3CN, DMF[79] and CH_2Cl_2/TBAP, calculated by using these equations, are summarized in Tables III and IV. In all of the solvents ΔG_{FET} is weakly exothermic and becomes *more* exothermic as $E_{1/2}(b/b^-)$ becomes less negative. By contrast, ΔG_{BET} is strongly exothermic and becomes *less* exothermic as $E_{1/2}(b/b^-)$ becomes less negative. The calculations also show that ΔG_{FET} varies by approximately 0.3 eV across the series while ΔG_{BET} spans a 0.8 eV range. The attenuated variation of ΔG_{FET} compared to ΔG_{BET} results from the fact that ΔG_{FET} depends on $E_{0,0}$ and the latter quantity varies substantially across the series.

Kinetics of Forward ET in (b)ReDMAB Complexes. The lifetimes of the MLCT emission (τ_{em}) for the two series of (b)ReL complexes at 25 °C in degassed CH_3CN, DMF, and CH_2Cl_2/TBAP solutions were measured by using time-correlated single photon counting (Table II). The emission lifetimes for the (b)ReB complexes vary from approximately 2 μs to 30 ns and are characteristic of the dπ (Re) → π* (diimine) MLCT excited state. Comparison of the emission energy and lifetime data for the (b)ReB complexes indicates that as E_{max} decreases, τ_{em} decreases. Correlation of τ_{em} and E_{max} has been studied extensively in families of Ru(II), Os(II), and Re(I) complexes; these studies have demonstrated that the effect is due to an increase the nonradiative decay rate as the excited-state energy decreases (energy gap law).[22,75]

The MLCT emission lifetime for each of the (b)ReDMAB complexes is substantially shorter than τ_{em} for the corresponding (b)ReB complex in the same solvent (Table II). The mechanism for the attenuation of τ_{em} in the (b)ReDMAB complexes is forward ET,

$$\underset{\text{MLCT}}{*[(b^{\bullet-})Re^{II}(CO)_3\text{-DMAB}]^+} \xrightarrow{k_{FET}} \underset{\text{LLCT}}{[(b^{\bullet-})Re^{I}(CO)_3\text{-DMAB}^{\bullet+}]^+} \quad (3)$$

which accelerates decay of the MLCT excited state by providing an additional nonradiative decay channel which is not available in the (b)ReB model complexes.[80] Support for this conclusion comes from transient absorption experiments which provide clear evidence for the ligand-to-ligand charge-transfer (LLCT) state which is produced by forward ET (vide infra).

Under the assumption that forward ET is irreversible, the rate (k_{FET}) can be calculated from emission lifetime data by using the following equation,[11,15,16]

$$k_{FET} = 1/\tau - 1/\tau_{model} \quad (4)$$

where τ and τ_{model} are the lifetimes of the (b)ReDMAB complex and the corresponding (b)ReB complex, respectively. Rate constants for forward ET in the (b)ReDMAB complexes in CH_3CN, DMF, and CH_2Cl_2/TBAP solutions at 25 °C, calculated from the emission lifetime data by using eq 4, are summarized in Table III. The k_{FET} values range from 10^7 s^{-1} to greater than 10^9 s^{-1}. For (bpz)ReDMAB and (deb)ReDMAB in CH_2Cl_2/TBAP, τ_{em} was too short to allow determination of k_{FET}. Two points are of interest with regard to the forward ET rate data. First, in all solvents, k_{FET} increases as ΔG_{FET} becomes more exothermic. Second, by comparing rates at comparable driving force, the following qualitative trend emerges: $k_{FET}(CH_2Cl_2/TBAP) > k_{FET}(DMF) > k_{FET}(CH_3CN)$. Both of these observations are consistent with the semiclassical theory of ET and will be discussed below.

The temperature dependence of k_{FET} was determined by measuring the emission lifetimes of the (b)ReDMAB and (b)ReB complexes in CH_3CN solution at seven temperatures over the range −5° to +45 °C. The rate constants at each temperature were calculated by using eq 4, and then the activation parameters for forward ET (ΔH^*_{FET} and ΔS^*_{FET}) were determined from Eyring plots of the data (Table III). The ΔH^*_{FET} values are comparatively small and decrease as ΔG_{FET} becomes more exothermic. By contrast, the ΔS^*_{FET} values are comparatively large and negative and are constant within experimental error across the series.

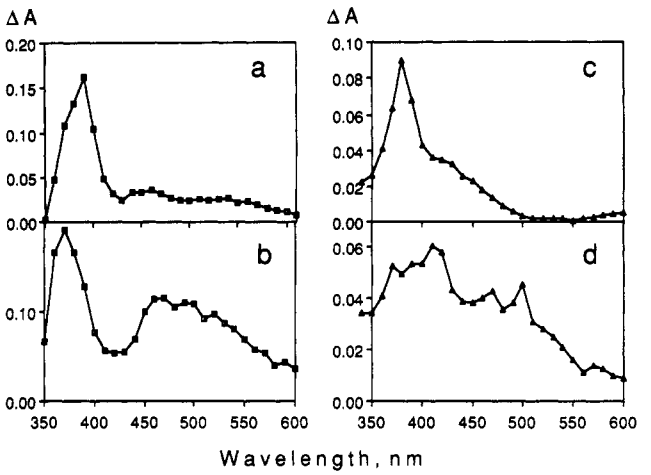

Figure 3. Transient absorption difference spectra of Re complexes in CH_2Cl_2/TBAP solution, 20-ns delay after 355-nm laser excitation (8 mJ, 6-ns fwhm): (a) (bpz)ReB, (b) (bpz)ReDMAB, (c) (tmb)ReB, (d) (tmb)ReDMAB.

Transient Absorption Spectroscopy: The LLCT State and Kinetics of Back ET. Nanosecond laser flash photolysis was conducted on the (b)ReL complexes in CH_3CN and CH_2Cl_2/TBAP by using the third harmonic of a Nd:YAG laser for excitation (355 nm, 6 ns fwhm, 8 mJ). All of the complexes display strong transient absorption in the wavelength range from 350 to 700 nm; however, the spectra of the (b)ReDMAB complexes differ significantly from those of the corresponding (b)ReB complexes.

The transient absorption difference (ΔA) spectra of (bpz)ReB and (tmb)ReB in CH_2Cl_2/TBAP are shown in Figure 3, a and c, respectively; these spectra are qualitatively similar to those observed for the other four (b)ReB complexes. The transient absorption spectra of the (b)ReB complexes are characteristic of the dπ (Re) → π* (diimine) MLCT excited state.[81] The strong near-UV absorption feature is likely due to spin-allowed π*,π* and/or π,π* absorption of the diimine radical anion. In accord with the MLCT assignment, the lifetimes of the transients observed by laser flash for the (b)ReB complexes in both solvents are the same, within experimental error, as the MLCT emission lifetimes (compare τ_{TA}, Table IV, with τ_{em}, Table II).

The transient absorption spectra of the (b)ReDMAB complexes were determined in CH_2Cl_2/TBAP and CH_3CN solution. Each compound displays an absorption band in the 450–550-nm range that is not present in the spectra of the corresponding (b)ReB complexes. This mid-visible absorption band is clearly seen in the spectra of (bpz)ReDMAB and (tmb)ReDMAB (Figure 3, b and d). The transient absorption spectra of the four other (b)ReDMAB complexes display similar absorption in the 450–550-nm region. The lifetimes of the transients produced by laser flash of the (b)ReDMAB complexes were determined by monitoring at 370 nm and 500 nm; the lifetimes at each wavelength are the same within experimental error (τ_{TA}, Table IV). Note that for each (b)ReDMAB complex, τ_{TA} is longer than the MLCT emission lifetime, but shorter than the lifetime of the MLCT state of the corresponding (b)ReB model complex.

The transient absorption spectra of the (b)ReDMAB complexes are assigned to the LLCT state, $[(b^{\bullet-})Re^{I}(CO)_3\text{-DMAB}^{\bullet+}]^+$, that is formed by forward ET, eq 3. This assignment is supported by several observations. First, the transients observed for the (b)-

(79) The DMAB/DMAB$^+$ couple is irreversible in DMF; the peak potential for the irreversible anodic wave ($E_{p,a}$) was used as an approximation for $E_{1/2}$.

(80) Low-temperature (77 K) emission studies of *N,N*-diethyl-*p*-(*N',N'*-dimethylamino)benzamide indicate that the singlet and triplet energies of the DMAB chromophore are 3.7 and 3.0 eV, respectively. Thus, energy transfer from the Re → diimine MLCT state (E < 2.7 eV) to the DMAB chromophore is endothermic for each (b)ReDMAB complex and would be quite slow.

(81) Tapolsky, G.; Duesing, R.; Meyer, T. J. *J. Phys. Chem.* **1989**, *93*, 3885.

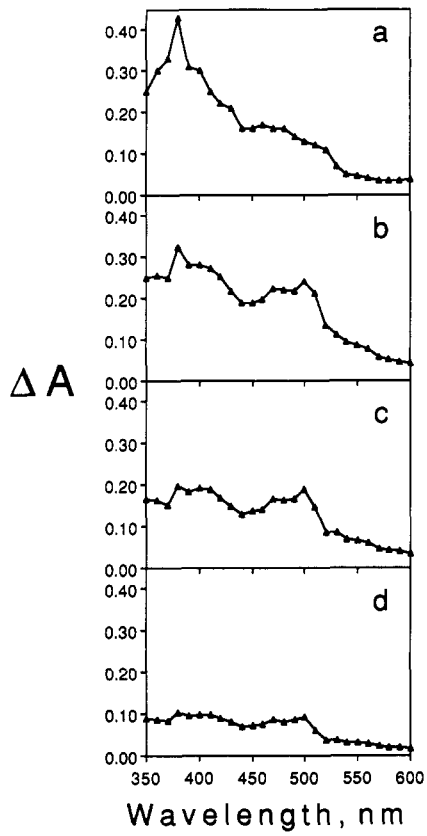

Figure 4. Transient absorption difference spectra of (tmb)ReDMAB in CH_3CN solution at various delay times following 355-nm excitation (8 mJ, 6-ns fwhm): (a) 20-ns delay, (b) 50-ns delay, (c) 200-ns delay, (d) 300-ns delay.

ReDMAB complexes are clearly not due to the MLCT state, since the lifetimes (τ_{TA}) are substantially longer than the MLCT emission lifetimes. Second, studies of substituted dimethylaniline radical cations in low-temperature glasses suggest that the DMAB radical cation ($DMAB^{\bullet+}$) should absorb near 500 nm.[82] Third, in several cases the transient absorption spectrum of the (b)-ReDMAB complex evolves in time from an initial spectrum, characteristic of the MLCT state, to a spectrum at a later time in which the mid-visible absorption band that is attributed to $DMAB^{\bullet+}$ has developed. This sequence is illustrated in Figure 4, which shows the transient absorption spectra of (tmb)ReDMAB in CH_3CN solution at four delay times following laser excitation. Significantly, the timescale for development of the 500-nm absorption band (20–50 ns) is consistent with the emission lifetime of the MLCT state (τ = 46 ns).

Since decay of the LLCT excited state occurs via back ET,

$$[(bpy^{\bullet-})Re^{I}(CO)_3\text{–}DMAB^{\bullet+}]^+ \xrightarrow{k_{BET}} [(bpy)Re^{I}(CO)_3\text{–}DMAB]^+ \quad (5)$$

the transient absorption decay lifetimes directly afford the rate of back ET (e.g., $k_{BET} = 1/\tau_{TA}$). The k_{BET} values for the (b)-ReDMAB complexes in CH_3CN and CH_2Cl_2/TBAP, calculated from the lifetime data, are listed in Table IV. Remarkably, k_{BET} *increases* as ΔG_{BET} becomes *less* exothermic.

Analysis of Forward ET Rates. Figure 5 shows plots of log k_{FET} as a function of ΔG_{FET} for the series of (b)ReDMAB complexes in three solvents. Although the data exhibit scatter, several conclusions can be drawn from these figures. First, the plots show that separate rate–exothermicity correlations exist for forward ET in each solvent. Second, in each solvent, k_{FET} increases as ΔG_{FET} becomes more exothermic. Third, by comparing rates at comparable driving force, the following qualitative trend emerges:

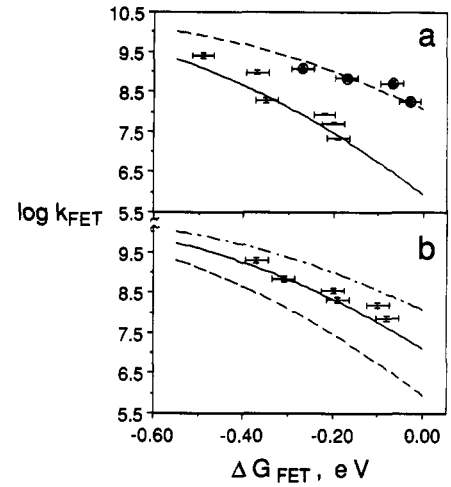

Figure 5. Forward ET rates for (b)ReDMAB complexes as a function of ΔG_{FET}. (a) Uncircled points with error bars, CH_3CN solution; circled points with error bars, CH_2Cl_2/TBAP solution; lines calculated using eq 6 with H_{AB} = 7 cm^{-1}; (—) λ = 1.0 eV; (- - -) λ = 0.8 eV. (b) Points with error bars represent data in DMF solution; lines calculated using eq 6 with H_{AB} = 7 cm^{-1}: (- - -) λ = 1.0 eV; (—) λ = 0.9 eV; (·····) λ = 0.8 eV.

$k_{FET}(CH_2Cl_2/TBAP) > k_{FET}(DMF) > k_{FET}(CH_3CN)$. We now turn to a discussion of ET theory in order to explain these observations.

The semiclassical theory expresses the ET rate constant as the product of a nuclear and an electronic transmission coefficient (κ_n and κ_{el}, respectively) and an effective nuclear-vibration frequency (ν_n):[83]

$$k_{ET} = \nu_n \kappa_{el} \kappa_n \quad (6a)$$

where

$$\nu_n \kappa_{el} = \left\{\frac{2H_{AB}^2}{h}\right\}\left\{\frac{\pi^3}{\lambda k_B T}\right\}^{1/2} \text{ and } \kappa_n = \exp\left\{-\frac{(\Delta G_{ET} + \lambda)^2}{4\lambda k_B T}\right\} \quad (6b)$$

In eq 6, H_{AB} is the donor–acceptor electronic coupling matrix element, λ is the total reorganization energy, ΔG_{ET} is the free-energy change for ET, and h, k_B, and T have their usual definitions. The semiclassical expression defines a quantitative relationship between k_{ET} and ΔG_{ET}, T, and parameters which are related to the structure of the donor, acceptor, and surrounding medium (e.g., H_{AB} and λ). This expression has been extremely successful in correlating rate data for a variety of weakly exothermic normal region ET reactions.[1a,1b,2,5,7]

If λ and H_{AB} are known, then the dependence of k_{ET} on ΔG_{ET} (and/or T) can be calculated by using eq 6; thus, to allow calculation of the predicted dependence of k_{FET} on ΔG_{FET} for the (b)ReDMAB system we have estimated λ and H_{AB}. Recent theoretical arguments suggests that when the overall entropy change for ET is small ($\Delta S° \approx 0$), the nuclear and electronic terms can be estimated from the apparent activation parameters ($\Delta H^{\ddagger}$ and $\Delta S^{\ddagger}$) by,[13b,84-86]

$$\ln \kappa_n \approx -\Delta H^{\ddagger}/RT \quad (7a)$$

$$\ln \kappa_{el} \approx \Delta S^{*}/R \quad (7b)$$

where $\Delta S^{*} \approx \Delta S^{\ddagger} - \Delta S^{*}_{FC}$ and $\Delta S^{*}_{FC} \approx 0.5\Delta S°$. Implicit in

(82) Forster, M.; Hester, R. E. *J. Chem. Soc., Faraday Trans. 2* **1981**, *77*, 1521.

(83) (a) Sutin, N. In ref 2, p 441. (b) Brunschwig, B.; Sutin, N. *Comments Inorg. Chem.* **1987**, *6*, 209.

(84) Sutin, N. In *Supramolecular Photochemistry*; Balzani, V., Ed.; D. Reidel: Dordrecht, 1987; p 173.

(85) Marcus, R. A.; Sutin, N. *Inorg. Chem.* **1975**, *14*, 213.

(86) Hupp, J. T.; Weaver, M. J. *Inorg. Chem.* **1984**, *23*, 256.

the use of eq 7b to calculate κ_{el} from the apparent activation entropy ($\Delta S^{\ddagger}$) is the assumption that the Franck–Condon activation entropy (ΔS^{*}_{FC}), which is proportional to ΔS° (see above expression), is negligible.[86] If this is the case, then $\Delta S^{\ddagger}$ directly provides a measure of the degree of nonadiabaticity for the ET reaction.

To establish the validity of the assumption that $\Delta S^{*}_{FC} \approx 0$ in the present system, ΔS° for forward ET (eq 3) was estimated by measuring the temperature dependence of the (bpy/bpy$^{\bullet-}$) and (DMAB/DMAB$^{\bullet+}$) redox couples in (bpy)ReDMAB by nonisothermal cyclic voltammetry. After taking into account the electronic spin-state change that accompanies relaxation of the predominantly triplet MLCT excited state,[87] ΔS° for forward ET is estimated to be $\approx +1.5$ eu. This suggests that for (bpy)ReDMAB, $\Delta S^{*}_{FC} \approx 0$, and thus $\Delta S^{*} \approx \Delta S^{\ddagger}$, within the limits of experimental error. Since the charge type for forward ET is the same for all of the (b)ReDMAB complexes, it is reasonable to assume that this approximation holds for the other diimine complexes as well.[88]

By using the $\Delta H^{\ddagger}_{FET}$ values for the (b)ReDMAB complexes in CH_3CN solution, eq 7a leads to an estimate of $\lambda \approx 1.0 \pm 0.1$ eV.[89] By taking $\lambda = 1.0$ eV and using the $\Delta S^{\ddagger}_{FET}$ values in CH_3CN solution (-13 ± 1 eu), eq 7b yields an estimate of $H_{AB} \approx 7$ cm^{-1}. Now, by taking these estimates for λ and H_{AB}, eq 6 was used to calculate the dependence of k_{FET} on ΔG_{FET} for CH_3CN solution. The line calculated using these parameters (solid line, Figure 5a) provides a reasonable fit to the rate data for CH_3CN solution. Furthermore, very good fits for the driving-force dependence of k_{FET} in CH_2Cl_2/TBAP and DMF solutions are obtained by using eq 6 with $H_{AB} = 7$ cm^{-1} and $\lambda = 0.8$ eV and 0.9 eV, respectively (see Figures 5 a and b). In summary, the dependence of k_{FET} on ΔG_{FET} suggests that λ is solvent dependent and that the electronic coupling is weak and apparently not solvent dependent.

The λ values obtained for forward ET in the (b)ReDMAB complexes contain components arising from both inner- and outer-sphere terms (λ_i and λ_o, respectively). Contributions to λ_i are expected from molecular reorganization that occurs within both the *[(b$^-$)Re^{II}(CO)$_3$] acceptor and the DMAB donor upon ET. By using the MOPAC semiempirical method (AM1 Hamiltonian) to calculate the difference in the heat of formation of the DMAB donor in its equilibrium nuclear geometry and in the equilibrium nuclear geometry of the radical cation, λ_i for the donor was estimated to be 0.15 eV.[90] The contribution to λ_i due to the *[(b$^-$)Re^{II}(CO)$_3$] acceptor can only be estimated by comparison with related systems. The change in electronic configuration for the excited-state reduction is $(d\pi)^5(\pi^*)^1$ to $(d\pi)^6(\pi^*)^1$; this process is isoelectronic with respect to the excited-state reduction of $Ru(bpy)_3^{2+}$, for which λ_i has been estimated to be <0.1 eV.[91] By analogy, we anticipate that λ_i for the excited-state Re acceptor center is quite small as well.[92] Taken together these approximations suggest that an upper limit for λ_i for forward ET is 0.25 eV.

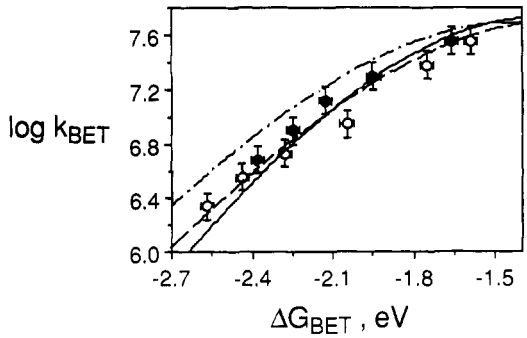

Figure 6. Back ET rates for (b)ReDMAB complexes as a function of ΔG_{BET}. Dark circles with error bars, CH_3CN solution; light circles with error bars, CH_2Cl_2/TBAP solution. Lines calculated by using eq 9 and 10 with the following parameters: (—) $N = 1$ (single high-frequency mode), $H_{AB} = 0.6$ cm^{-1}, $\hbar\omega_c = 1500$ cm^{-1}, $S_c = 3.5$, $\lambda_s = 0.75$ eV; (- - -) $N = 2$ (two high-frequency modes), $H_{AB} = 0.6$ cm^{-1}, $\hbar\omega_{c1} = 1500$ cm^{-1}, $S_{c1} = 2.0$, $\hbar\omega_{c2} = 2500$ cm^{-1}, $S_{c2} = 0.8$, $\lambda_s = 0.75$ eV; (····) same as (- - -) except $\lambda_s = 0.9$ eV.

The two-sphere dielectric continuum model can be used to estimate the contribution of λ_o to the observed λ,[38-41]

$$\lambda_o = e^2\left[\frac{1}{2r_D} + \frac{1}{2r_A} - \frac{1}{r_{DA}}\right]\left[\frac{1}{\epsilon_{op}} - \frac{1}{\epsilon_s}\right] \qquad (8)$$

where e is the electron charge, r_D and r_A are the radii of the donor and acceptor, respectively, r_{DA} is the donor–acceptor separation distance, and ϵ_{op} and ϵ_s are the optical and static dielectric constants, respectively. By using estimates for the radii of the DMAB donor and the Re(I) acceptor (3.2 Å and 4.0 Å, respectively)[93] and the Re to DMAB separation distance (10 Å), eq 8 leads to the following calculated values of λ_o: 0.99 eV (CH_2Cl_2), 1.20 eV (DMF), and 1.37 eV (CH_3CN). Summing the values for λ_i and λ_o leads to estimated upper limits for the total reorganization energy for the (b)ReDMAB complexes in the three solvents examined: 1.25 eV (CH_2Cl_2), 1.45 eV (DMF), and 1.62 eV (CH_3CN).

Several comments should be made concerning the experimental and calculated values for the reorganization energy. First, in each case the calculated λ values are approximately 50% larger than the experimental values. One possible reason for this discrepancy could be that the calculated ΔG_{FET} values contain a systematic error—a shift in the absolute value of ΔG_{FET} for each complex would lead to a commensurate shift in λ. However, in a recent comparison of λ values for a series of ligand-bridged Ru dimers, it was found that the values calculated by using the two-sphere dielectric continuum expression (eq 8) were consistently 20%–30% larger than experimental values determined from intervalence charge-transfer absorption maxima.[41a] Interestingly, for the ligand-bridged dimers which have a metal–metal separation distance of 10–11 Å, λ values range from 1.1 to 1.3 eV (H_2O solution).[41a] These values are in reasonable agreement with the experimental λ for the (b)ReDMAB complexes in CH_3CN, especially in light of the fact that λ should be larger in H_2O compared to CH_3CN.

The second point is that the experimental rate data for forward ET clearly suggest that λ follows the trend $CH_3CN > DMF > CH_2Cl_2$. The ratio of the λ values determined from the fits of the rate data (Figure 5) is 1.0 (CH_3CN):0.9 (DMF):0.8 (CH_2Cl_2). The ratio which is calculated by using eq 8, 1.0 (CH_3CN):0.85 (DMF):0.73 (CH_2Cl_2), is in reasonable agreement with the experimental ratio. Thus, the solvent dependence of λ provides an explanation for the fact that for comparable ΔG_{FET}, k_{FET} follows the trend $CH_2Cl_2 > DMF > CH_3CN$. Note that the solvent dependence of λ has a significant effect on the ET rates: for $\Delta G_{FET} \approx -0.2$ eV, the 20% decrease in λ that accompanies a change in

(87) Kober, E. M.; Meyer, T. J. *Inorg. Chem.* **1984**, *23*, 3877.
(88) Hupp, J. T.; Weaver, M. J. *Inorg. Chem.* **1984**, *23*, 3639.
(89) The assumption made in this calculation is that $\Delta H^{\ddagger}_{FET} \approx \Delta G^{\ddagger} = (\Delta G_{FET} + \lambda)^2/4\lambda$.
(90) (a) Dewar, M. J. S.; Zoebisch, E. G.; Healy, E. F.; Stewart, J. P. *J. Am. Chem. Soc.* **1985**, *107*, 3902. (b) Stewart, J. P. *MOPAC Manual: A General Molecular Orbital Package*, Energetics Division, Directorate of Chemical Sciences, Frank J. Seiler Research Laboratory, Publication No. FJSRL-TR-0007, 1988.
(91) Toma, H. E.; Creutz, C. *Inorg. Chem.* **1977**, *16*, 545.
(92) A reviewer pointed out that because of the effect of the strongly back-bonding CO ligands, λ_i for reduction of the *[(b$^-$)Re^{II}(CO)$_3$] acceptor may be larger than for reduction of *[Ru^{II}(bpy)$_3$]$^{2+}$. Unfortunately, little information is available concerning the effect of intraligand reorganization on λ_i for redox processes of transition metal complexes (ref 1a, pp 278–279). However, we note that the ΔG dependence of the rate of reductive bimolecular quenching of *fac*-[(bpy)Re(CO)$_3$(NCCH$_3$)]$^+$ by a series of aromatic amines in CH_3CN (Perkins, T. A.; Schanze, K. S. Unpublished.) closely follows the correlation observed in a study of the reductive quenching of *[Ru^{II}(bpy)$_3$]$^{2+}$ by the same aromatic amines in CH_3CN (ref 7). The correspondence of the ΔG dependence for reductive quenching of the two excited states supports the hypothesis that λ_i is small for reduction of the *[(b$^-$)Re^{II}(CO)$_3$] acceptor.
(93) The molecular radii were estimated by using the expression $r = (3V/4\pi)^{1/3}$, where V is the molecular volume within the van der Waals surface, calculated by using the CALCULATE VOLUME command in the SYBYL program.

solvent from CH_3CN to CH_2Cl_2 leads to an increase in k_{FET} by a factor of 10.

Analysis of Back ET Rates. Figure 6 shows a plot of log k_{BET} as a function of ΔG_{BET} for the series of (b)ReDMAB complexes in CH_3CN and CH_2Cl_2/TBAP. The observed rates display an inverted free-energy dependence; however, k_{BET} changes by only a factor of ≈40 for a 1.0-eV variation in ΔG_{BET}. This dependence of the rate on driving force is weaker than in other systems in which the inverted region effect has been observed.[9,10,54,55,57,58] We turn to a discussion of the quantum theory of ET processes to seek an explanation for this observation.

Because of the importance of nuclear tunnelling in highly exothermic ET reactions, an expression which includes contributions from quantized high-frequency acceptor modes must be used to fit rate data, rather than the semiclassical expression (eq 6). In the case of highly exothermic ET reactions, the theoretical approach begins with the Fermi golden rule expression,[83,94,95]

$$k_{ET} = \frac{2\pi}{\hbar} H_{AB}\langle FC\rangle \qquad (9)$$

where the rate is given by the product of an electronic term (H_{AB}) and a Franck–Condon nuclear term (FC). In a commonly used approximation, the Franck–Condon term is derived by assuming that a single low-frequency ($\hbar\omega_s$) and several medium- and/or high-frequency modes ($\hbar\omega_{ci}$) are coupled to ET.[95] In this approximation, the low-frequency (solvent) mode is treated as a classical harmonic oscillator and the high-frequency modes are treated as quantized harmonic oscillators. When the low-frequency mode is in the high-temperature limit and the high-frequency modes are in the low-temperature limit ($\hbar\omega_s \ll k_BT \ll \hbar\omega_{ci}$), the following expression is obtained:[95]

$$FC = \frac{\exp\{-\sum_{i=1}^{N} S_{ci}\}}{(4\pi\lambda_s k_B T)^{1/2}} \sum_{w_1=0}\sum_{w_2=0}\cdots \sum_{w_N=0}\prod_{i=1}^{N}\frac{(S_{ci})^{w_i}}{w_i!} \exp\left\{\frac{-(\Delta G_{ET} + \lambda_s + \sum_{i=1}^{N} w_i\hbar\omega_{ci})^2}{4\lambda_s k_B T}\right\} \qquad (10)$$

In eq 10, $\hbar\omega_{ci}$ is the frequency and S_{ci} is the unitless displacement for the ith high-frequency-mode ($S_{ci} = \lambda_{ci}/\hbar\omega_{ci}$), λ_s is the reorganization energy for the low-frequency mode, and the summations are taken over the quantum levels (w_N) of the high-frequency modes.

Equations 9 and 10 have frequently been applied to the analysis of experimental rate data for highly exothermic, inverted region ET under the assumption that the high-frequency acceptor modes can be represented as a single mode (e.g., $N = 1$ in eq 10) with an average frequency ($\hbar\omega_c$) and average displacement, S_c (where $S_c = \lambda_c/\hbar\omega_c$).[8-10,43,54,58] The single high-frequency mode analysis has been used to fit the rate data for back ET in the (b)ReDMAB complexes; the solid line in Figure 6 was generated by using eq 9 and 10 with $N = 1$, $H_{AB} = 0.6$ cm^{-1}, $\lambda_s = 0.75$ eV, $\hbar\omega_c = 1500$ cm^{-1}, and $S_c = 3.5$ ($\lambda_c = 0.65$ eV). While it is important to realize that this analysis simply represents a four-parameter fit of the experimental rate data, several of the parameters are physically reasonable. First, $\hbar\omega_c = 1500$ cm^{-1} was selected based on the hypothesis that diimine and DMAB based C–C stretching modes are the dominant high-frequency modes displaced concomitant to back ET. Second, λ_s was adjusted to a value that is close to the value observed for forward ET. Finally, S_c and H_{AB} were adjusted to optimize the fit. It is important to note that there is little "interaction" between these parameters: S_c affects the slope and H_{AB} displaces the line along the vertical axis.

The value of H_{AB} required to fit the data is approximately an order of magnitude smaller than the electronic coupling for forward ET. This is not surprising, since back ET essentially involves transfer of charge from the diimine ligand to the DMAB moiety; the donor and acceptor sites are separated by ≈9 Å, their π systems are orthogonal, and the intervening Re center may not facilitate electronic coupling. The unusual feature is the comparatively large value of S_c required to fit the rate data: S_c = 3.5 ($\lambda_c = 0.65$ eV) is considerably larger than expected for back ET. (The large S_c is required because of the weak dependence of k_{BET} on ΔG_{BET}).

Scheme II

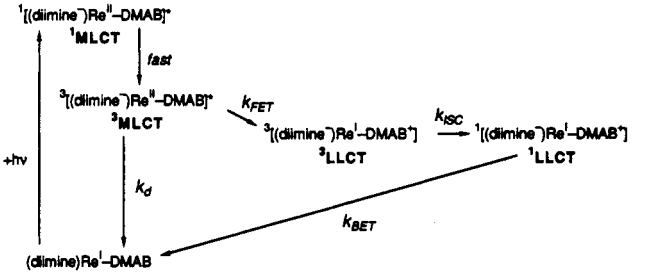

One possible reason for the comparatively weak dependence of k_{BET} on ΔG_{BET} in the (b)ReDMAB complexes is that, in addition to the diimine and DMAB based C–C stretching modes, high-frequency modes associated with the metal center (such as the C–O stretching modes of the carbonyl ligands) may be displaced concomitant to ET. It is reasonable to expect that such vibronic modes will respond to back ET, because in the intermediate LLCT state, the odd electron occupies an orbital which has some density at the metal center (e.g., $\Psi = \psi_{\pi^*bpy} + \xi\psi_{d\pi Re}$).

To demonstrate the effect that another set of high-frequency modes will have on the dependence of k_{BET} on ΔG_{BET}, the experimental data have been fitted by using eq 9 and 10 with two-high frequency modes. The dashed line in Figure 6 was calculated with the parameter set: $N = 2$, $H_{AB} = 0.6$ cm^{-1}, $\lambda_s = 0.75$ eV, $\hbar\omega_{c1} = 1500$ cm^{-1}, $S_{c1} = 2.0$ ($\lambda_{c1} = 0.37$ eV), $\hbar\omega_{c2} = 2500$ cm^{-1}, $S_{c2} = 0.8$ ($\lambda_{c2} = 0.24$ eV). As can be seen, these parameters provide a good fit to the experimental data. This analysis demonstrates that coupling another set of moderately displaced high-frequency modes to back ET acts to "flatten" the dependence of k_{BET} on ΔG_{BET} in the inverted region.

While the above analysis provides an explanation for the relatively weak dependence of k_{BET} on ΔG_{BET}, two alternative explanations must be considered. First, the analysis based on eq 9 and 10 assumes that H_{AB} remains constant across the series. This assumption may not be valid for the series of (b)ReDMAB complexes. Superexchange theory suggests that for a spacer-mediated electron-transfer mechanism (as opposed to a hole-transfer mechanism), $H_{AB} \propto 1/\Delta E_{DS}$, where ΔE_{DS} is the energy gap between the HOMO of the donor site and the LUMO of the spacer.[27,31,33-35] For back ET in the (b)ReDMAB complexes, the donor HOMO energy (the diimine radical anion) follows the trend tmb > dmb > bpy > dab > deb > bpz; superexchange theory predicts that H_{AB} will follow the same trend. If this is the case, with increasing exothermicity, H_{AB} *increases* while the Franck–Condon factors *decrease*. Because of the opposing trends in the two terms, the dependence of k_{BET} on ΔG_{BET} will be attenuated. Evidence for variation of H_{AB} as a function of ΔG_{BET} may come from temperature-dependence studies, which are currently in progress.

A second alternative explanation is that intersystem crossing (ISC), rather than back ET, is the rate-determining step for decay of the LLCT state. An excited-state diagram which includes the possible effect of ISC on the decay of the LLCT state is shown in Scheme II. Initial excitation of the (b)Re(CO)$_3$ chromphore produces ^{1}MLCT, which rapidly relaxes to ^{3}MLCT.[87] Since the excited state which precedes forward ET is ^{3}MLCT, conservation of spin during ET will produce ^{3}LLCT. As a result, before back ET can occur, ^{3}LLCT must undergo ISC (with rate k_{ISC}) to ^{1}LLCT. If $k_{ISC} \ll k_{BET}$, ISC will be rate determining, and the observed decay rate will correspond to k_{ISC} instead of k_{BET}. If this is the case, then it should be possible to explain the observed

(94) Ulstrup, J. *Charge Transfer Processes in Condensed Media*; Springer-Verlag: Berlin, 1979.
(95) Ulstrup, J.; Jortner, J. *J. Chem. Phys.* **1975**, *63*, 4358.

variation of the decay rate of the LLCT state in terms of the effect that $E_{1/2}(b/b^-)$ has on k_{ISC}. As pointed out above, in the LLCT state the odd electron occupies an MO which can be represented as $\Psi = \psi_{\pi^*diimine} + \xi\psi_{d\pi Re}$. Since the energy of the diimine π^* level (ϵ_{π^*}) is greater than that of the $d\pi$ Re levels, perturbation theory indicates that ξ will decrease as ϵ_{π^*} increases.[96] Stated in other terms, as $E_{1/2}(b/b^-)$ becomes more negative (ϵ_{π^*} increases), the extent of mixing of the π^* (diimine) MO and the $d\pi$ (Re) MO decreases (ξ decreases). From this argument, it follows that in the LLCT state, the degree of metal character in the MO which the odd electron occupies increases in the following manner: tmb < dmb < bpy < dab < deb < bpz. Now comes the explanation for the effect of $E_{1/2}(b/b^-)$ on k_{ISC}. It is reasonable to expect that k_{ISC} will increase as ξ increases, because spin–orbit coupling should increase as the degree of metal character in the MO which the odd electron occupies increases.[97] From the above argument, since ξ increases as $E_{1/2}(b/b^-)$ becomes less negative, it follows that k_{ISC} will increase along the series tmb < dmb < bpy < dab < deb < bpz, in accord with the experimentally observed trend in the decay rate of the LLCT state.

Finally, note that for the (b)ReDMAB series, the dependence of k_{BET} on ΔG_{BET} seems to follow the same correlation for CH_3CN and CH_2Cl_2/TBAP (see Figure 6). Both the semiclassical and quantum theories qualitatively predict that in the inverted region, for a given ΔG_{ET}, k_{ET} will increase as solvent polarity increases. An estimate of the effect of solvent polarity on k_{BET} in the (b)-ReDMAB system has been calculated by using the quantum expression. The dashed–dotted line in Figure 6 was generated by using eq 9 and 10 with the same parameters as for the dashed line (see above), but λ_s was increased from 0.75 eV to 0.90 eV. The 20% increase in λ_s is predicted by the two-sphere model (eq 8) for a change from CH_2Cl_2 to CH_3CN. As can be seen from Figure 6, this calculation suggests that the effect of solvent polarity on k_{BET} will be comparatively small. Because of the relatively small solvent effect that is expected, it is possible that different rate/free-energy correlations are not observed for the two solvents due to error in the measurements.[98]

Comparison of ET Rate Data with Other Systems. A. Forward ET. It is of interest to compare the forward ET rates for the (b)ReDMAB complexes with rates of photoinduced ET in other compounds. In two covalently linked porphyrin–quinone (P–Q) systems, the dependence of k_{ET} on ΔG_{ET} has been determined in sufficient detail to allow estimation of the optimal rate constant ($\nu_n\kappa_{el}$, eq 6) for ET from the photoexcited porphyrin to the quinone acceptor. In one P–Q system, a Zn–tetraphenylporphyrin (Zn-TPP) donor is linked to a series of quinone acceptors via a trypticene spacer.[59b] The approximate center-to-center separation distance is 10 Å; however, only one saturated (sp^3) carbon atom separates the conjugated π systems of ZnTPP and the quinone, and the through-space distance between the π systems is $\approx$ 2.5 Å. A value of $\nu_n\kappa_{el} = 3 \times 10^{11}$ s^{-1} is estimated for this system.[59b] In another P–Q compound, a Zn *meso*-phenyloctamethylporphyrin is linked to a series of quinones via a bicyclo[2.2.2]octane spacer. In this system, the center-to-center and through-space separation distances are 16 Å and 5.6 Å, respectively, and $\nu_n\kappa_{el}$ is estimated to be 1.5×10^{10} s^{-1}.[16]

The value of $\nu_n\kappa_{el}$ in the (b)ReDMAB series (1.4×10^{10} s^{-1}) is comparable to that of the bicyclooctane bridged P–Q system, which suggests that electronic coupling is similar in the two systems. This is surprising, since only one saturated (sp^3 hybridized) atom lies between the π-electron systems of the DMAB donor and the Re acceptor, while four saturated atoms comprise the bicyclooctane spacer. One possible reason for the weak coupling in the (b)ReDMAB system could be that overlap between the metal-based acceptor orbital (5d with π symmetry) and the intervening spacer orbitals (π^* pyridyl, π^* N—C═O, etc.) is poor.

A point to consider in making these comparisons is that, during forward ET, the electron is transferred from the photoexcited porphyrin to the quinone (photooxidation),[16,59] while in the (b)-ReDMAB system the electron is transferred from DMAB to the photoexcited metal (photoreduction). This difference might lead to a difference in the predominant superexchange path for electronic coupling.[8,27] In the P–Q systems, coupling via vacant spacer orbitals may predominate (electron transfer path), and in the (b)ReDMAB system, coupling via filled spacer orbitals may predominate (hole transfer path). Studies of long-range ET in metalloproteins and in P–Q compounds have provided some evidence that the "directionality" of photoinduced ET may influence the magnitude of spacer-mediated electronic coupling.[19b,63]

B. Back ET. In other systems in which the Marcus inverted region effect has been observed, the dependence of k_{ET} on ΔG_{ET} is stronger than in the (b)ReDMAB series.[54,55,57,58] Most rate data on inverted region ET have been obtained with organic donor–acceptor systems. The Franck–Condon analysis presented above suggests that one possible explanation for the difference in inverted region behavior between the Re complexes and the organic systems is that there are fewer high-frequency acceptor modes available in the organic compounds. If this analysis is correct, it places significant limitations on the design of molecular devices which can be used to generate long-lived charge-separated states. This is because the analysis suggests that when the structure of a molecular system allows coupling of many high-frequency modes to a highly exothermic charge–recombination reaction, the Franck–Condon factors are more favorable for the energy-wasting back ET reaction.

Conclusion and Summary

Rates for photoinduced forward and back ET have been determined in the series of (b)ReDMAB complexes in solvents of differing polarity. The free-energy dependence of the weakly exothermic forward ET reaction correlates well with nonadiabatic semiclassical rate theory. The data analysis suggests that the total reorganization energy decreases as the solvent polarity decreases, leading to significantly faster charge separation in less polar media. The highly exothermic back ET reaction displays a weakly inverted dependence of the rate on free energy. Several possible explanations for the weak free-energy dependence are considered including participation of metal-complex-based high-frequency acceptor modes in addition to diimine- and DMAB-based C–C stretching modes, variation of electronic coupling with ΔG_{BET}, and the possibility that intersystem crossing is the rate-determining step for decay of the LLCT state.

Acknowledgment. Acknowledgment is made to the donors of the Petroleum Research Fund, administered by the American Chemical Society, for support of this work. The transient absorption experiments were performed at the Center for Fast Kinetics Research, which is supported jointly by the Biomedical Research Technology Program of the Division of Research Resources of the National Institutes of Health (RR00886) and by The University of Texas at Austin. We thank Ms. Dorothy M. Freeto for travel support. Special thanks go to Professor T. J. Meyer for helpful discussions concerning analysis of the back ET rate data.

(96) Albright, T. A.; Burdett, J. K.; Whangbo, M.-H. *Orbital Interactions in Chemistry*; Wiley: New York, 1985.

(97) Turro, N. J. *Modern Molecular Photochemistry*; Benjamin/Cummings: Menlo Park, CA, 1978.

(98) Close inspection of Figure 6 reveals that for most of the data points (at similar ΔG_{BET}) k_{BET} is slightly larger in CH_3CN; however, it is difficult to resolve a different correlation for the two solvents due to experimental error.